ESC HEART FAILURE
ESC Heart Failure 2017; **4**: 241–251
Published online 3 April 2017 in Wiley Online Library (wileyonlinelibrary.com) **DOI:** 10.1002/ehf2.12154

ORIGINAL RESEARCH ARTICLE

Local microRNA-133a downregulation is associated with hypertrophy in the dyssynchronous heart

Lars B. van Middendorp[1,2]*, Marion Kuiper[1], Chantal Munts[1], Philippe Wouters[1], Jos G. Maessen[2], Frans A. van Nieuwenhoven[1] and Frits W. Prinzen[1]

[1]*Department of Physiology, Cardiovascular Research Institute Maastricht, Maastricht University, Maastricht, Limburg, The Netherlands;* [2]*Department of Cardiothoracic Surgery, Cardiovascular Research Institute Maastricht, Maastricht University, Maastricht, Limburg, The Netherlands*

Abstract

Aims Left bundle branch block (LBBB) creates considerable regional differences in mechanical load within the left ventricle (LV). We investigated expression of selected microRNAs (miRs) in relation to regional hypertrophy and fibrosis in LBBB hearts and their reversibility upon cardiac resynchronization therapy (CRT).

Methods and results Eighteen dogs were followed for 4 months after induction of LBBB, 10 of which received CRT after 2 months. Five additional dogs served as control. LV geometric changes were determined by echocardiography and myocardial strain by magnetic resonance imaging tagging. Expression levels of miRs, their target genes: connective tissue growth factor (CTGF), serum response factor (SRF), nuclear factor of activated T cells (NFATc4), and cardiomyocyte diameter and collagen deposition were measured in the septum and LV free wall (LVfw). In LBBB hearts, LVfw and septal systolic circumferential strain were 200% and 50% of control, respectively. This coincided with local hypertrophy in the LVfw. MiR-133a expression was reduced by 33% in the LVfw, which corresponded with a selective increase of CTGF expression in the LVfw (279% of control). By contrast, no change was observed in SRF and NFATc4 expression was decreased in LBBB hearts. CRT normalized strain patterns and reversed miR-133a and CTGF expression towards normal, expression of other miRs, related to remodelling, such as miR-199b and miR-155f, were not affected.

Conclusions In the clinically relevant large animal model of LBBB, a close inverse relation exists between local hypertrophy and miR-133a. Reduced miR-133a correlated with increased CTGF levels but not with SRF and NFATc4.

Keywords MicroRNAs; Connective tissue growth factor; Dyssynchrony; Hypertrophy/remodelling; Cardiac resynchronization therapy

Received: 6 September 2016; Revised: 18 January 2017; Accepted: 22 February 2017
**Correspondence to: Lars B. van Middendorp, Department of Physiology, Cardiovascular Research Institute Maastricht, Maastricht University, Universiteitssingel 50, P.O. Box 616, 6200 MD Maastricht, The Netherlands. Tel: +31 43 3881086; Fax: +31 43 3884166. Email: l.vanmiddendorp@maastrichtuniversity.nl*

Introduction

Both mechanical and humoral triggers have been proposed to explain the hypertrophic and fibrotic response in cardiac muscle exposed to excessive load. However, *in vivo*, it is difficult to separate the contribution of (local) mechanical load and (systemic) neurohumoral activation, because global cardiac overload, as in hypertension and valvular disease, also leads to neurohumoral stimulation/activation. On the other hand, it has been shown that stretching isolated cardiomyocytes can affect gene expression, increase protein synthesis, and induce hypertrophy.[1] Similarly, stretching isolated cardiac fibroblasts increases expression of extracellular matrix (ECM) genes and proteins.[2,3]

Dyssynchronous electrical activation of the heart, such as during left bundle branch block (LBBB), creates discoordinate contraction of the left ventricle (LV). This discoordination leads to elevated mechanical load in the LV free wall (LVfw) and reduced load in the septum.[4,5] Animal studies have shown complex changes in myocardial tissue of dyssynchronous hearts, including extensive regional differences in tissue growth (hypertrophy) and in expression of hundreds of genes.[4–6] Therefore, LBBB provides an interesting *in vivo* condition that allows to investigate the sequelae of different loading conditions within the same heart and to distill the effect of local load from that of systemic components that are presumably equal throughout the heart. Moreover, local abnormalities

can be largely corrected by cardiac resynchronization therapy (CRT).

In the process of cardiac hypertrophy and fibrosis, several microRNAs (miRs) play an important role.[7–10] miR-1, miR-133a, miR-155f, and miR-199b have been linked to cardiac hypertrophy,[11–14] while miR-29c and miR-30c were described in cardiac fibrosis.[15–17] Furthermore, miR-146a, miR-146b, miR-222, and miR-499 were included in the analysis.[18] It is unclear to what extent the expression of these miRs is regulated by local load or by systemic factors.

It was the aim of the present study to investigate whether in hearts with LBBB, the local changes in mechanical load translate into regional differences in expression of miRs as well as hypertrophy and fibrosis. Furthermore, the reversibility of dyssynchrony-induced structural and molecular changes was analysed after normalization of local mechanical load by CRT.

Methods

Animal handling was performed according to the Dutch Law on Animal Experimentation and the European Directive for the Protection of Vertebrate Animals used for Experimental and Other Scientific Purposes (86/609/EU). The protocol was approved by the Experimental Animal Committee of Maastricht University.

Experimental models

Experiments were performed on 23 adult mongrel dogs of either sex, weighing approximately 20 kg. Five dogs served as control. The other 18 dogs underwent a sterile closed-chest procedure. They were intravenously induced with thiopental (500 μg), and anaesthesia was maintained by continuous infusion of midazolam (0.25 mg/kg/h) and sufentanil (3 μg/kg/h). LBBB was induced by radiofrequency ablation as described in detail previously.[19] In 10 of these dogs, a CRT device (Consulta CRT-P, Medtronic, Minneapolis, MN, USA) was implanted during the same procedure. All leads were placed endovascularly under fluoroscopic guidance. The LV lead was preferably placed in a (postero-)lateral vein. The right ventricular (RV) lead was positioned in the RV apex, and an atrial lead was placed in the right atrial auricle. The CRT device was initially set to sensing only. Two months after LBBB induction, the biventricular pacemaker was programmed to DDD, using a relatively short atrio-ventricular (AV)-delay to ensure complete capture by LV and RV pacing. Dogs underwent awake echocardiography exams at baseline, after 2 months, just prior to switching on the CRT device and at sacrifice to assess wall thickness and end diastolic volume (EDV). A few days before sacrifice, cine magnetic resonance imaging scans (Intera 1.5Tesla MRI, Philips, Amsterdam, The Netherlands) were made under anaesthesia, to measure LV wall volume, end systolic volume, and EDV. The same anaesthetic protocol was used as for induction of LBBB. Myocardial tissue tagging scans were made for calculation of circumferential strain using the Sinmod programme.[20] At the final day of the experimental protocol, 4 months after LBBB induction, extensive electro-haemodynamic measurements were performed as described in detail previously.[21] Subsequently, the heart was rapidly excised, and transmural tissue sections at the mid-level from the LVfw and septum were collected and snap-frozen in liquid nitrogen for further analysis. Part of the tissue was preserved using formalin for histology. The five dogs that served as control were only subjected to a magnetic resonance imaging scan and electro-haemodynamic measurements, before collecting the tissue.

RNA analysis

Total RNA was isolated from tissue using Qiagen miR mini easykit (Qiagen, Venlo, the Netherlands). Quantity and purity of RNA were assed using the ratio of absorbance at 260/280 nm, by means of a nanodrop 2000c spectrophometer (Wilmington, DE, USA). RNA was reverse transcribed to cDNA using miScript reverse transcription kit (Qiagen, Venlo, the Netherlands). MiR expression was analysed using real-time quantitative PCR on an iCycler real-time PCR detection system using the iQ SYBR-green supermix (Bio-Rad, Veenendaal, the Netherlands). MiR expressions were normalized for the reference miR: let-7f, and their relative expression was calculated using the comparative threshold cycle (Ct) method by calculating $2^{\Delta Ct}$ (e.g. $2^{\text{let-7f Ct} - \text{miR-133a Ct}}$). Expression levels of connective tissue growth factor (CTGF), serum response factor (SRF), nuclear factor of activated T cells (NFATc4), collagen type 1 (COL1A1), and brain natriuretic peptide were analysed using the same method. They were normalized using the housekeeping gene cyclophilin-A, and their relative expression was calculated using the comparative Ct method by calculating $2^{\Delta Ct}$ (e.g. $2^{\text{Cyclophilin Ct} - \text{CTGF Ct}}$). The sequences of the specific primers used can be found in the Supporting Information (*Table S1*).

Cardiac collagen content and cardiomyocyte diameter

The acid-soluble collagen content of frozen LV and septal transmural tissue samples was examined using the Sircol collagen assay (Biocolor Ltd., Belfast, UK). The volume percentage of collagen in cardiac tissue was histologically determined in tissue sections stained with 0.1% Sirius Red.[22] Images were taken with a Leica DM3000 Microscope (Leica Mircosystems, Wetzlar, Germany). Custom made software within Matlab (MathWorks, Natick, MA, USA) was

used to calculate percentage of collagen after manually selecting the region of interest and adjusting the threshold. Perivascular collagen was excluded from the analysis. For each dog on average, eight tissue sections per cardiac wall segment were analysed. Cardiomyocyte diameter at the level of the nucleus was determined using ImageJ (Research Services Branch, National Institute of Mental Health, MA, USA) in tissue sections after a modified azan staining. On average 30 cardiomyocytes per cardiac wall segment were analysed.

Statistical analysis

Data are presented as median [25th–75th percentile]. Statistical analysis was performed using Statistical Package for Social Sciences for Windows version 20.0 (IBM corp., Armonk, NY, USA). Differences between groups, temporal differences within a group and, when applicable, intracardiac differences were tested with a mix-effect analysis. This method is also known as multilevel analysis or linear mixed effect model and was used for gene expression levels, electro-haemodynamic parameters, and imaging data. The least squared differences correction was used for post hoc comparison. A Pearson correlation linear regression analysis between expression levels of different mRNAs and miRs was performed. An observed probability value <0.05 was considered statistically significant.

Results

LBBB induces cardiac dyssynchrony and dysfunction, which is partly reversed by CRT

Electro-haemodynamic measurements showed that LBBB caused a ~35% decrease in LV dP/dt_{max} together with an almost doubling of QRS width (*Table 1*). Mechanical interventricular dyssynchrony, the time difference of the upslope of normalized LV and RV pressure,[19] became more negative upon LBBB, indicating earlier contraction of the RV than of the LV. CRT reduced QRS width, increased LV dP/dt_{max} and mechanical interventricular dyssynchrony to values in between control and LBBB (*Table 1*).

LBBB increases local strain in LVfw, which is partly reversed by CRT

In the control group, circumferential strain was similar in the septum and the LVfw. In the LBBB group, LVfw circumferential

Table 1. Electro-haemodynamic parameters at baseline and after 4 months of remodelling (chronic)

	4 months LBBB		2 months LBBB ➔ 2 months CRT		
	Baseline	Chronic	Baseline	Chronic, CRT-off	Chronic, CRT-on
Haemodynamic					
Heart rate (bpm)	84 [70–102]	100 [96–110]*	101 [99–102]***	100 [100–100]	100 [100–100]
LV dP/dt_{max} (mmHg/s)	1713 [1502–1863]	1097 [1009–1282]*	1954 [1622–2269]	1249 [1038–1591]*	1411 [1107–1735]*,**
LV dP/dt_{min} (mmHg/s)	−1989 [−1673 to −2162]	−1569 [−1373 to −1715]*	−1982 [−1912 to −2277]	−1649[−1558 to −1744]*	−1820 [−1599 to −1987]*,**,***
LV end systolic pressure (mmHg)	102 [95–112]	89 [87–108]	103 [99–110]	91 [87–95]*	90 [87–95]*
LV end diastolic pressure (mmHg)	6 [3–7]	6 [5–11]	8 [4–11]	6 [5–8]	5 [3–7]
RV end systolic pressure (mmHg)	23 [20–24]	25 [24–27]	28 [24–36]	27 [25–30]	26 [24–29]
RV end diastolic pressure (mmHg)	4 [2–4]	5 [4–5]	5 [2–12]	5 [4–6]	4 [4–6]
Mechanical interventricular dyssynchrony (ms)	−7 [−3 to −9]	−46 [−37 to −50]*	−6 [−4 to −11]	−42 [−30 to −43]*	−26 [−19 to −33]*,**,***
ECG					
PQ time (ms)	133 [125–155]	167 [137–191]	134[123–159]	150 [133–180]	67 [62–71]*,**,***
QRS width (ms)	51 [48–59]	100 [97–106]*	48 [47–51]	102 [98–110]*	89 [85–94] *,**,***
QT width (ms)	335 [302–346]	352 [346–381]*	318 [309–330]	382 [370–385]*	367 [351–377]*

CRT, cardiac resynchronization therapy; ECG, electrocardiogram; LBBB, left bundle branch block; LV, left ventricle; RV, right ventricle.
In case of the LBBB+CRT group, the data at baseline, and during CRT are shown as well as during CRT temporarily switched off. Significance is placed behind the 75th percentile.
*$P < 0.05$ chronic vs. baseline.
**$P < 0.05$ CRT-off vs. CRT-on.
***$P < 0.05$ LBBB+CRT vs. LBBB group. Presented are median [25th–75th percentile] values.

DOI: 10.1002/ehf2.12154

strain was twice as high as in the control LVfw, while strain in the septum was reduced by half. CRT restored the strain patterns to near normal levels (*Figure 1*).

Magnetic resonance imaging-derived LV EDV was slightly but significantly higher in the LBBB than in the control group, while LV EDV in the LBBB+CRT group was not significantly different from the control group. In the LBBB group, LV wall volume was significantly (42%) higher than in the control group, while this difference was less in the LBBB+CRT group (27% compared with control; *Figure 1*).

LBBB induces local LVfw hypertrophy, which is partly reversed by CRT

In the LBBB group, LVfw wall thickness increased by 18% within 4 months, while septal wall thickness did not significantly change. In the LBBB+CRT group, CRT equalized LVfw and septal wall thickness (*Figure 2*). The ratio of wall thickness of the LVfw and septum, an index of asymmetry of hypertrophy, was 1.06 [0.98–1.11] at baseline, increased significantly after LBBB to 1.28 [1.15–1.36] and returned to 1.07 [0.95–1.11] after 2 months of CRT. Echo-derived

Figure 1 Magnetic resonance imaging-derived left ventricular (LV) volumes and strains at the end of the protocol (at 4 months) in the three groups: control; left bundle branch block (LBBB) and LBBB + cardiac resynchronization therapy (CRT). Panel (A) LV end diastolic volume (EDV); panel (B) LV wall volume. Panels (C), (D), and (E) typical examples of strain patterns in control, LBBB, and CRT septum (dashed lines) and LV free wall (LVfw; solid lines). Note the discoordinated contraction during LBBB with pre-stretch of the LVfw (1) and septal rebound stretch (2). Time of aortic valve opening (AvO) and closure (AvC) are depicted by dashed vertical lines. Panel (F) circumferential strain in the septum and LVfw as percentage of mean strain of the total LV. In panels (A), (B), and (F), the line within each box indicates the median value, the upper and lower margins of the box, the 25th–75th percentile, and the bars the minimum and maximum value. *$P < 0.05$ vs. equivalent region in control; †$P < 0.05$ vs. septum in same heart; ‡$P < 0.05$ vs. same region in LBBB group.

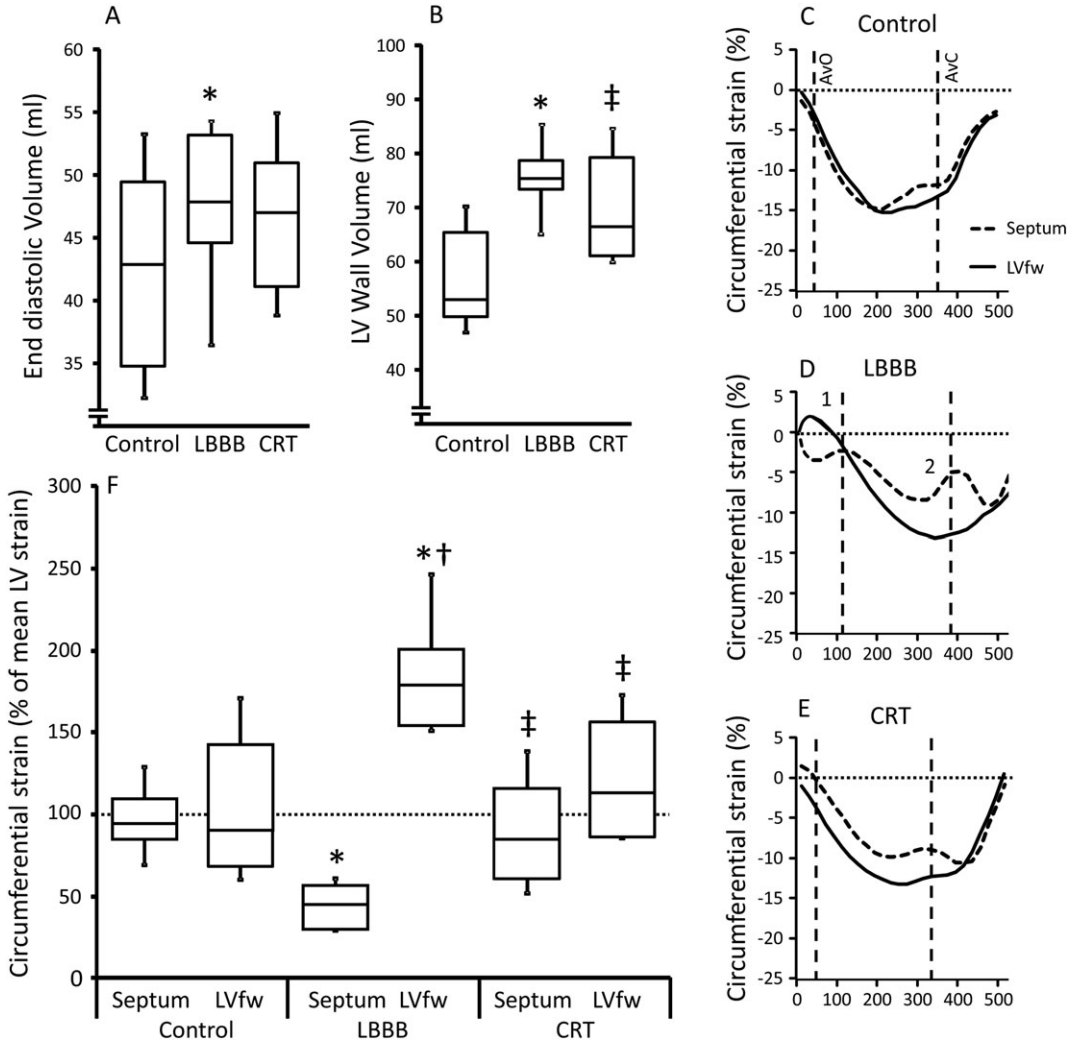

DOI: 10.1002/ehf2.12154

Figure 2 Left ventricular geometric changes due to left bundle branch block (LBBB) and LBBB + cardiac resynchronization therapy (CRT), expressed as percentage change from baseline. Panel (A) wall thickness of the septum (circles) and left ventricular free wall (LVfw; squares) in LBBB (black filled symbols) and LBBB+CRT (open symbols) dogs. Panel (B) LVfw/septal wall thickness ratio in LBBB (black filled symbols) and LBBB+CRT (open symbols) dogs. Panel (C) end diastolic volume in LBBB (black filled symbols) and LBBB+CRT (open symbols) dogs. *$P < 0.05$ vs. baseline (month 0); †$P < 0.05$ vs. month 2; ‡$P < 0.05$ vs. LBBB. Presented are median values and 25th or 75th percentile to on-side only for clarity.

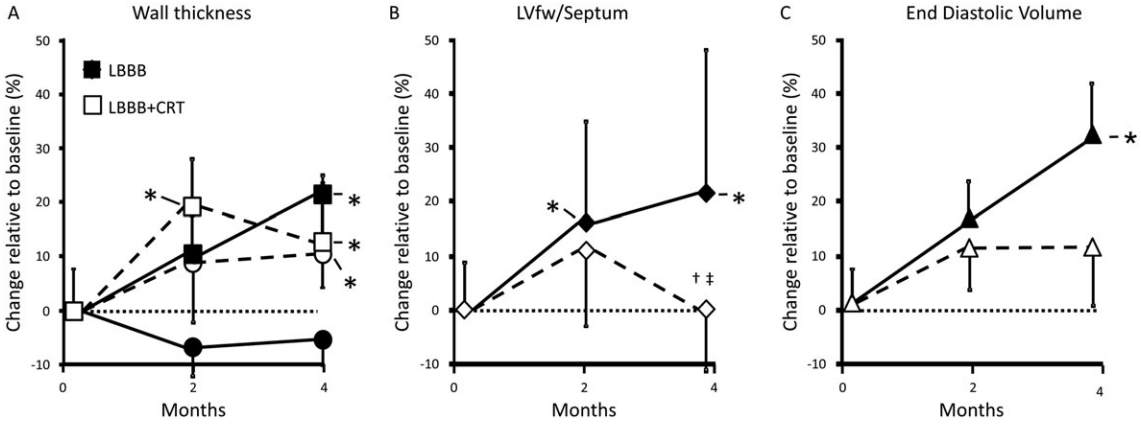

EDV increased slightly after 2 months of LBBB in the LBBB and LBBB+CRT groups. In the LBBB group, EDV continued to increase and was, after 4 months, significantly larger than in the control group. In the LBBB+CRT group, no further increase in EDV was found after starting CRT (*Figure 2*).

The increased wall thickness in the LVfw of LBBB hearts, observed by the echocardiographic measurements, was corroborated by the histologically measured cardiomyocyte diameter, which was significantly larger in the LVfw than in the septum (*Figure 3*). The ratio of cardiomyocyte diameter of the LVfw and septum was 0.95 [0.90–1.03] in the control

Figure 3 Panel (A) representative examples of the modified azan staining in the septum and left ventricular free wall (LVfw) in the same heart of a LBBB dog (magnification is equal between the slices). Panel (B) cardiomyocyte diameter in the septum and LVfw in the control, left bundle branch block (LBBB), and LBBB + cardiac resynchronization therapy (CRT) group. Data in panel (B) are presented as median (the line within each box), the upper and lower margins of the box are the 25th–75th percentile and the bars the minimum and maximum value, *$P < 0.05$ vs. corresponding region in control; †$P < 0.05$ vs. septum in the same heart.

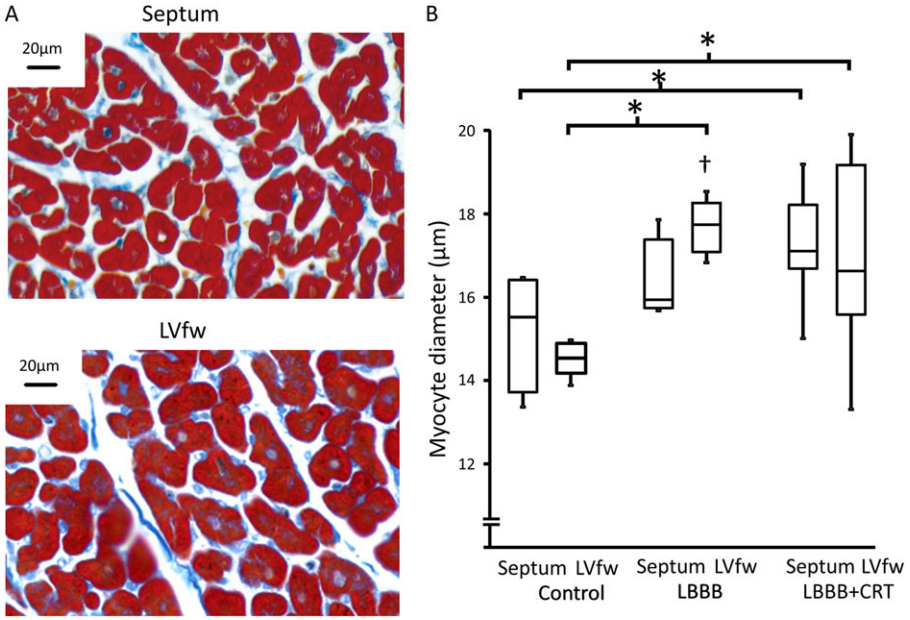

DOI: 10.1002/ehf2.12154

group, was significantly elevated (1.08 [1.03–1.13]) in the LBBB group and was 1.00 [0.88–1.09] in the LBBB+CRT group.

LBBB induces local downregulation of left ventricular free wall miR-133a expression, which is partly reversed by CRT

MiR-1 and miR-133a were by far the most abundantly expressed miRs (*Table 2*), and the expression levels of other miRs that have been associated with cardiac hypertrophy were much lower.

In the LBBB group, expression of miR-133a was significantly reduced by 33% in the LVfw, while septal miR-133a expression was similar to control. In the LBBB+CRT group, miR-133a values in both the LVfw and septum were not significantly different from control (*Figure 4*). MiR-155f levels were marginally increased only in LVfw of LBBB+CRT hearts; miR-199b showed small but significant lower levels in the LBBB and LBBB+CRT hearts. miR-1, miR-146a, miR-146b, miR-222, and miR-499 expression levels in LBBB and LBBB+CRT hearts were not significantly different from control (*Table 2*).

In the hypertrophied LVfw of the LBBB group median, CTGF expression was 279% of control, which was significantly higher than the expression in the septum (119% of control). In LBBB+CRT hearts, CTGF overexpression was more similar in the LVfw and septum (229% and 141% of control, respectively; *Figure 4*). The CTGF LVfw/septum ratio tended to be higher in the LBBB (1.7 [1.2–2.5]) than in the control (1.2 [0.7–1.40, $P = 0.07$]). This ratio was not significantly different between LBBB+CRT and control (1.2 [1.1–2.4] $P = 0.39$). The expression of SRF was similar in all groups. NFATc4 expression was very low and was decreased in LBBB hearts (both septum and LVfw).

Brain natriuretic peptide was hardly expressed in any of the groups and was not significantly different between the groups (*Table 2*).

Cardiac collagen content and related miR expression

The biochemical Sircol assay as well as the histological Sirius Red measurements indicated a tendency for a ~15% lower collagen concentration in the LVfw of the LBBB group ($P = 0.06$), while collagen was similar in all other investigated samples (*Figure 5*). In both the LBBB and LBBB+CRT groups, COL1A1 expression was significantly below control in both LV walls. MiR-29c and miR-30c expression levels were similar in all groups (*Figure 5*).

Relation of miR-133a with CTGF, SRF and NFATc4 expression

Plotting the mRNA expression of CTGF, SRF, and NFATc4 (all three known target genes of miR-133a) as a function of miR-133a showed a significant inverse correlation between miR-133a and CTGF (*Figure 6*). No significant correlation was observed between miR-133a and SRF or NFATc4 (*Figure 6*).

Discussion

This large animal model of LBBB provides the unique opportunity to study the involvement of local mechanical load in processes related to hypertrophy and fibrosis. Development of local hypertrophy in the LVfw during LBBB coincided with local down-regulation of miR-133a and up-regulation of CTGF. Together with the observation that local hypertrophy, miR-133a, and CTGF expression were reversible upon CRT, these data indicate that hypertrophy is regulated locally in LBBB. By contrast, collagen gene expression level was reduced in the entire LV and was not reversible upon CRT. Therefore, collagen synthesis is either regulated by systemic factors or is so sensitive to abnormal strain patterns that it remains abnormal while being subjected to the only moderately abnormal strains during CRT.

MiR-133a expression in asymmetric hypertrophy and its reversal

MiR-133 is one of the most highly expressed miRs in cardiac tissue (*Table 2*). MiR-133 is down-regulated during cardiac hypertrophy, and miR-133 inhibition induced cardiac hypertrophy while miR-133 overexpression markedly reduced the hypertrophic response.[12] These previous findings support our finding that miR-133a is closely related to cardiac hypertrophy. The specificity of the relation between miR-133a, CTGF, and asymmetric hypertrophy in LBBB hearts is further emphasized by the lack of local overexpression of miR-199b and miR-155f, which are often up-regulated during pressure overload and concentric hypertrophy.[13,14] These results from a clinically relevant large animal model support the concept that miR-133a plays an important role in the hypertrophic response of cardiomyocytes under conditions of increased myocardial strain. Previous studies have already linked the local hypertrophy in the late-activated regions of dyssynchronous hearts to the locally increased strain and workload.[5,23] The coincidence of increased systolic strain, reduced miR-133a, and hypertrophy in the LVfw of LBBB hearts in the present study supports this view as well as the role of miR-133a in this process.

Table 2. Delta-CT of tested microRNAs (miR) and CTGF, NFATc4, SRF,COL1A1, and BNP

	Control		LBBB		LBBB+CRT	
microRNA	Septum	LVfw	Septum	LVfw	Septum	LVfw
miR-1	1.21 [0.90–1.37]	1.14 [1.02–0.17]	1.28 [0.83–0.79]	1.07 [0.79–0.37]	1.18 [0.82–0.45]	1.10 [0.63–0.37]
miR-29c	0.16 [0.12–0.21]	0.18 [0.16–0.21]	0.19 [0.18–0.23]	0.18 [0.15–0.21]	0.20 [0.17–0.23]	0.19 [0.16–0.21]
miR-30c	0.16 [0.14–0.25]	0.17 [0.14–0.19]	0.19 [0.15–0.21]	0.18 [0.14–0.21]	0.19 [0.17–0.23]	0.18 [0.14–0.19]
miR-133a	4.58 [3.23–5.72]	3.76 [3.37–4.03]	3.29 [2.87–4.16]	2.53 *,** [2.21–3.03]	3.09 [2.26–4.39]	2.85 [2.57–3.28]
miR-146a	0.0053 [0.0046–0.0057]	0.0049 [0.0048–0.0064]	0.0054 [0.0044–0.0066]	0.0059 [0.0047–0.0077]	0.0058 [0.0053–0.0070]	0.0068 [0.0056–0.0082]
miR-146b	0.0017 [0.0016–0.0019]	0.0021 [0.0017–0.0027]	0.0019 [0.0015–0.0021]	0.0029 [0.002–0.0048]	0.0021 [0.0014–0.0026]	0.0026 [0.0021–0.0038]
miR-155f	0.0029 [0.0027–0.0035]	0.0028 [0.0026–0.0040]	0.0039 [0.0029–0.0042]	0.0034 [0.0026–0.0054]	0.0036 [0.0028–0.0038]	0.0038** [0.0035–0.0052]
miR-199b	0.018 [0.016–0.021]	0.022** [0.020-0.026]	0.014 [0.011–0.015]	0.014*[0.01–0.023]	0.011* [0.01–0.015]	0.012* [0.01–0.016]
miR-222	0.086[0.083–0.102]	0.083 [0.073–0.097]	0.088 [0.077–0.105]	0.069 [0.062–0.104]	0.086 [0.078–0.097]	0.082 [0.072–0.096]
miR-499	0.33 [0.23–0.40]	0.32 [0.25–0.37]	0.27 [0.2–0.35]	0.31 [0.23–0.38]	0.25 [0.22-0.3]	0.28 [0.19-0.34]
mRNA						
CTGF	0.79 [0.62–0.85]	0.71 [0.48–1.14]	0.94 [0.81–1.99]	1.97*,** [1.41–2.75]	1.12 [0.58–1.64]	1.62* [0.99–2.63]
NFATc4	0.076 [0.067–0.112]	0.076 [0.071–0.132]	0.045* [0.033–0.068]	0.061* [0.043–0.068]	0.046* [0.035–0.067]	0.071 [0.065–0.111]
SRF	2.45 [1.61–2.66]	1.92 [1.89–0.3]	1.41 [1.36–0.67]	1.53 [0.97–0.81]	1.62 [1.32–0.08]	1.90 [1.55–0.2]
COL1A1	1.44 [1.08–1.76]	2.0** [1.71–2.39]	0.67* [0.46–1.22]	0.83*,** [0.66–1.30]	0.65* [0.41–0.80]	1.08** [0.84–1.55]
BNP	0.09 [0.06–0.13]	0.09 [0.02–0.29]	0.05 [0.02–0.09]	0.08 [0.04–0.15]	0.12 [0.06–0.23]	0.05 [0.02–0.12]

CT, threshold cycle; CTGF. connective tissue growth factor; COL1A. collagen type 1; NFATc4. nuclear factor of activated T cells; SRF. serum response factor.
Values are presented as median [25th–75th percentile]. Significance is placed behind the median value.
*$P < 0.05$ vs. control same region.
**$P < 0.05$ vs. septum of the same heart.

Figure 4 Relative miR-133a [panel (A)] and connective tissue growth factor (CTGF) expression [panel (B)] in the septum and left ventricular free wall (LVfw) in the control, left bundle branch block (LBBB), and LBBB + cardiac resynchronization therapy (CRT) group. Data are presented as median (the line within each box), the upper and lower margins of the box are the 25th–75th percentile and the bars the minimum and maximum value. *$P < 0.05$ vs. equivalent region in control; †$P < 0.05$ vs. septum in the same heart.

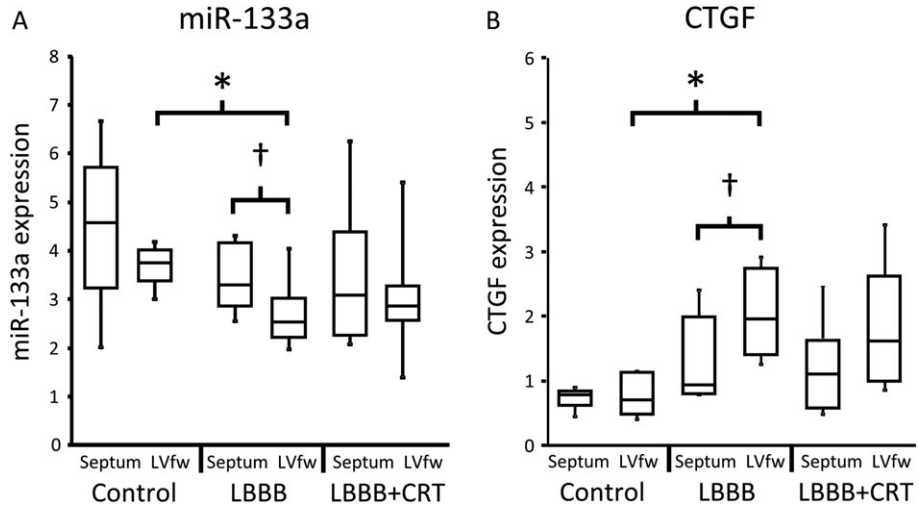

Figure 5 Relative expression of miR-29c [panel (A)], miR-30c [panel (B)], and collagen type 1 [COL1A1; panel (C)] in the septum and left ventricular free wall (LVfw) in the control, left bundle branch block (LBBB), and LBBB + cardiac resynchronization therapy (CRT) group. Relative change in collagen concentration based on the Sircol assay [panel (D)] and on Sirius Red histology [panel (E)], with representative examples of septal and LVfw sections of a LBBB dog [panel (F)]. Data in panels (A–E) are presented as median (the line within each box), the upper and lower margins of the box are the 25th–75th percentile, and the bars the minimum and maximum value, *$P < 0.05$ vs. equivalent region in control.

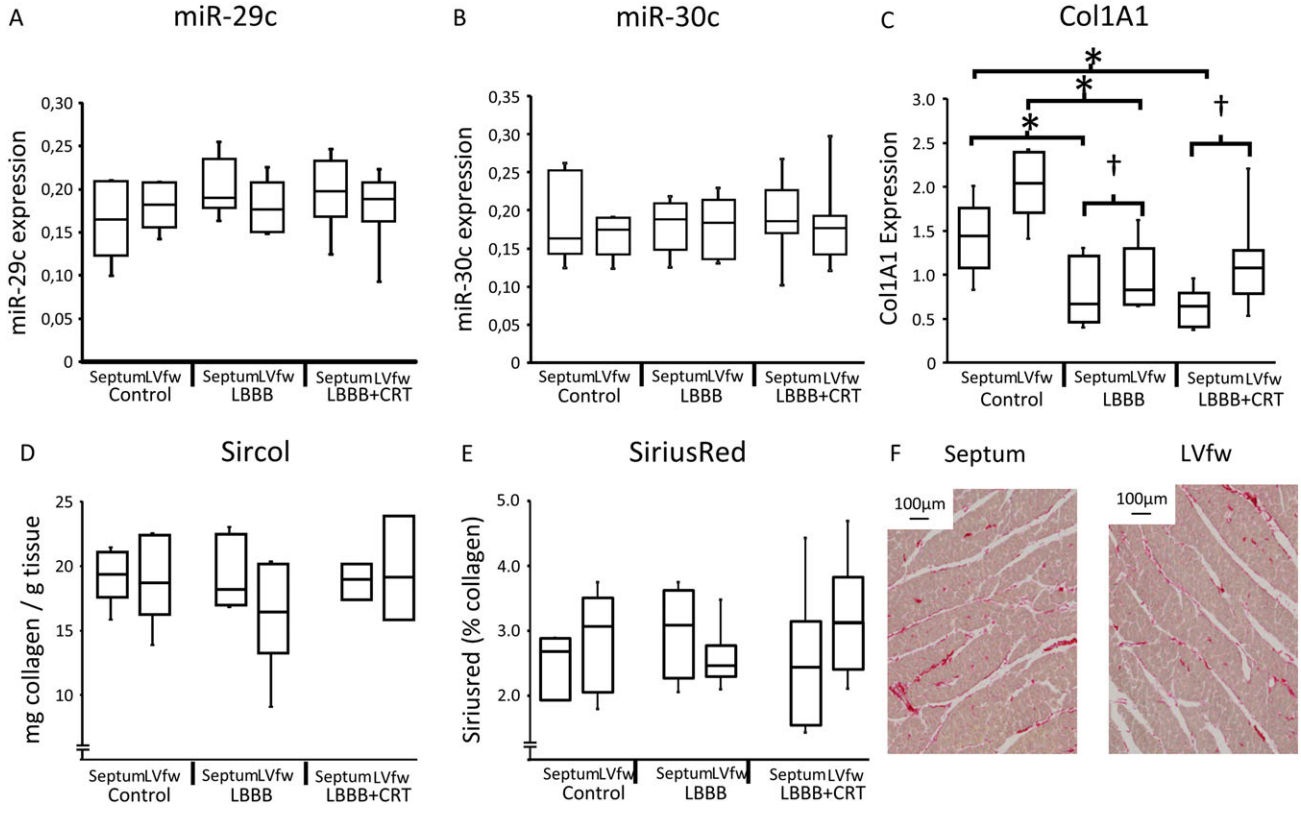

DOI: 10.1002/ehf2.12154

Figure 6 Relation between expression of miR-133a and its target genes connective tissue growth factor [CTGF; panel (A)], nuclear factor of activated T cells [NFATc4; panel (B)], and serum response factor [SRF; panel (C)]. Squares, control; triangles, left bundle branch block (LBBB); diamonds, cardiac resynchronization therapy (CRT) group. Solid symbols, left ventricular free wall; open symbols, septum. Pearson *r* and *P* values are based on all the individual data points; for clarity, only median values and 25th–75th percentile (bars) are depicted.

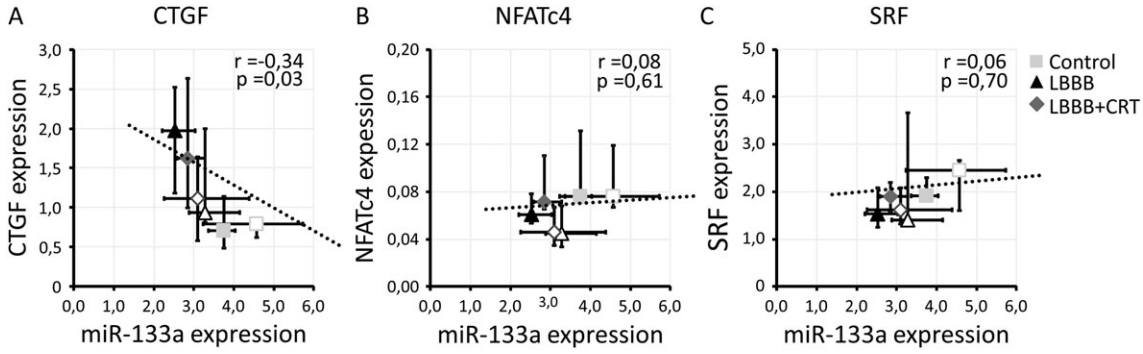

The present study corroborates the negative regulation of CTGF expression by miR-133a, observed in studies in isolated cardiomyocytes.[17] By contrast, SRF and NFATc4 (both known target genes of miR-133a) did not show any relation with miR-133a in this study and are most likely not involved in the hypertrophic response in our model of local hypertrophy. *In vitro* studies showed that increased CTGF expression in isolated, stretched cardiomyocytes coincided with development of a hypertrophic response.[1,3] Moreover, in a rabbit model of eccentric hypertrophy, where strains and workload are expected to be high throughout the LV wall, CTGF was also found to be overexpressed.[3] Of note is that recent studies question the importance of CTGF in cardiac structural remodelling, indicating that while it is an important biomarker of myocardial remodelling, it most likely does not play a decisive role in this process[24,25]

Cardiac collagen content

During the 4-month experimental period, LBBB did not lead to significant ECM remodelling and fibrosis, as collagen content remained similar and collagen gene expression showed a decrease. Possibly, the slightly lower collagen content in the LVfw of LBBB hearts may be explained by 'dilution' of collagen by the increased cardiomyocyte mass, as also shown in previous studies with chronic LV pacing.[4,5]

A remarkable observation in the present study is that the reduction in collagen expression did not occur locally but fairly uniform throughout the LV wall and that CRT did not reverse it. First of all, this emphasizes the completely different regulation of the processes of hypertrophy and ECM remodelling in LBBB hearts. Two explanations may be given. First of all, systemic factors may affect the anti-fibrotic events during LBBB, but in that case one should assume that these factors are not (completely) reversible upon CRT. Such incomplete recovery at the level of the entire LV wall is also supported by the incomplete return of LV cavity and wall volume to baseline levels upon CRT. COL1A1 is not the only factor that does not show local differences in expression in the dyssynchronous heart and that does not recover upon CRT. Studies have shown that, in hearts with LBBB and heart failure, a number of proteins and genes behave similarly.[6,26] The incomplete recovery upon CRT may simply indicate that conditions during CRT are still inferior to those with an intact ventricular conduction system. A second explanation may be that COL1A1 expression is influenced by myocardial stretch in specific parts of the cardiac cycle, such as early systole. In that phase, both early-activated and late-activated regions may be stretched during LBBB (*Figure 1*).[27] Such forms of stretch may also persist during CRT, because CRT does not completely normalize myocardial strains.[28]

A recent publication showed miR-30d expression data in the canine model of dyssynchronous heart failure (induced by rapid pacing and LBBB). In that animal model, miR-30d expression was increased in all myocardial samples from LBBB and CRT hearts, with higher miR-30d values in the LVfw of LBBB hearts, as well as some recovery by CRT.[29] The discrepancy with our data may be explained by sequence differences, or the absence of overt heart failure in our study, where the hypertrophy can be regarded as compensatory.

Limitations

Local workload was not directly measured in the present study. However, in LBBB hearts, systolic strain is a good indicator of local workload, because shortening against a (high, systolic) pressure determines external myocardial work and similar distribution of systolic strain and stress–strain loop area have been reported before.[30]

Conclusions

These data from a clinically relevant large animal model indicate a strong association between local cardiac mechanical load, down-regulation of miR-133a, and myocardial hypertrophy, all of which are reversible by CRT. These results obtained under *in vivo* conditions of LBBB and CRT indicate that hypertrophy and fibrosis are regulated by different triggers and along different pathways.

Conflicts of interest

F.W.P. has received research grants from Medtronic, St. Jude Medical, Sorin, MSD, and Biotronik.

Funding

This research was performed within the framework of CTMM, the Center for Translational Molecular Medicine (www.ctmm.nl), project COHFAR (grant 01C-203), and supported by the Dutch Heart Foundation.

Supporting information

Additional Supporting Information may be found online in the supporting information tab for this article.

Table S1. Specific primers used for real time quantitative PCR. For CTGF, BNP and Col1A1 both forward (fw) and reverse (rv) primers were used from Sigma-Aldrich (St. Louis, MO, USA). MicroRNA primers were obtained from Qiagen (Venlo, the Netherlands).

Table S2. Individual Let7f Ct values for each animal.

Figure S1. Ct values of Let7f in the septum and left ventricular free wall (LVfw) in the control, Left Bundle Branch Block (LBBB) and LBBB + Cardiac Resynchronization Therapy (CRT) group. Data are presented as median (the line within each box), the upper and lower margins of the box are the 25th-75th percentile and the bars the minimum and maximum value.

References

1. Blaauw E, van Nieuwenhoven FA, Willemsen P, Delhaas T, Prinzen FW, Snoeckx LH, van Bilsen M, van der Vusse GJ. Stretch-induced hypertrophy of isolated adult rabbit cardiomyocytes. *American Journal of Physiology Heart and Circulatory Physiology.* 2010; **299**: H780–H787.
2. Husse B, Briest W, Homagk L, Isenberg G, Gekle M. Cyclical mechanical stretch modulates expression of collagen I and collagen III by PKC and tyrosine kinase in cardiac fibroblasts. *American Journal of Physiology Regulatory, Integrative and Comparative Physiology.* 2007; **293**: R1898–R1907.
3. Blaauw E, Lorenzen-Schmidt I, Babiker FA, Munts C, Prinzen FW, Snoeckx LH, van Bilsen M, van der Vusse GJ, van Nieuwenhoven FA. Stretch-induced upregulation of connective tissue growth factor in rabbit cardiomyocytes. *Journal of Cardiovascular Translational Research.* 2013; **6**: 861–869.
4. van Oosterhout MF, Prinzen FW, Arts T, Schreuder JJ, Vanagt WY, Cleutjens JP, Reneman RS. Asynchronous electrical activation induces asymmetrical hypertrophy of the left ventricular wall. *Circulation.* 1998; **98**: 588–595.
5. Vernooy K, Verbeek XA, Peschar M, Crijns HJ, Arts T, Cornelussen RN, Prinzen FW. Left bundle branch block induces ventricular remodelling and functional septal hypoperfusion. *European Heart Journal.* 2005; **26**: 91–98.
6. Barth AS, Aiba T, Halperin V, DiSilvestre D, Chakir K, Colantuoni C, Tunin RS, Dimaano VL, Yu W, Abraham TP, Kass DA, Tomaselli GF. Cardiac resynchronization therapy corrects dyssynchrony-induced regional gene expression changes on a genomic level. *Circulation Cardiovascular Genetics.* 2009; **2**: 371–378.
7. Castaldi A, Zaglia T, Di Mauro V, Carullo P, Viggiani G, Borile G, Di Stefano B, Schiattarella GG, Gualazzi MG, Elia L, Stirparo GG, Colorito ML, Pironti G, Kunderfranco P, Esposito G, Bang ML, Mongillo M, Condorelli G, Catalucci D. MicroRNA-133 modulates the beta1-adrenergic receptor transduction cascade. *Circ Res.* 2014; **115**: 273–283.
8. Kumarswamy R, Thum T. Non-coding RNAs in cardiac remodeling and heart failure. *Circ Res.* 2013; **113**: 676–689.
9. Papait R, Greco C, Kunderfranco P, Latronico MV, Condorelli G. Epigenetics: a new mechanism of regulation of heart failure? *Basic Research in Cardiology.* 2013; **108**: 361.
10. Ohtani K, Dimmeler S. Control of cardiovascular differentiation by microRNAs. *Basic Research in Cardiology.* 2011; **106**: 5–11.
11. Vegter EL, van der Meer P, de Windt LJ, Pinto YM, Voors AA. MicroRNAs in heart failure: from biomarker to target for therapy. *European Journal of Heart Failure.* 2016; **18**: 457–468.
12. Care A, Catalucci D, Felicetti F, Bonci D, Addario A, Gallo P, Bang ML, Segnalini P, Gu Y, Dalton ND, Elia L, Latronico MV, Hoydal M, Autore C, Russo MA, Dorn GW 2nd, Ellingsen O, Ruiz-Lozano P, Peterson KL, Croce CM, Peschle C, Condorelli G. MicroRNA-133 controls cardiac hypertrophy. *Nature Medicine.* 2007; **13**: 613–618.
13. Heymans S, Corsten MF, Verhesen W, Carai P, van Leeuwen RE, Custers K, Peters T, Hazebroek M, Stoger L, Wijnands E, Janssen BJ, Creemers EE, Pinto YM, Grimm D, Schurmann N, Vigorito E, Thum T, Stassen F, Yin X, Mayr M, de Windt LJ, Lutgens E, Wouters K, de Winther MP, Zacchigna S, Giacca M, van Bilsen M, Papageorgiou AP, Schroen B. Macrophage microRNA-155 promotes cardiac hypertrophy and failure. *Circulation.* 2013; **128**: 1420–1432.
14. da Costa Martins PA, Salic K, Gladka MM, Armand AS, Leptidis S, el Azzouzi H, Hansen A, Coenen-de Roo CJ, Bierhuizen MF, van der Nagel R, van Kuik J, de Weger R, de Bruin A, Condorelli G, Arbones ML, Eschenhagen T, De Windt LJ. MicroRNA-199b targets

the nuclear kinase Dyrk1a in an auto-amplification loop promoting calcineurin/NFAT signalling. *Nature Cell Biology*. 2010; **12**: 1220–1227.
15. Thum T. Noncoding RNAs and myocardial fibrosis. *Nature Reviews Cardiology*. 2014; **11**: 655–663.
16. van Rooij E, Sutherland LB, Thatcher JE, DiMaio JM, Naseem RH, Marshall WS, Hill JA, Olson EN. Dysregulation of microRNAs after myocardial infarction reveals a role of miR-29 in cardiac fibrosis. *Proceedings of the National Academy of Sciences of the United States of America*. 2008; **105**: 13027–13032.
17. Duisters RF, Tijsen AJ, Schroen B, Leenders JJ, Lentink V, van der Made I, Herias V, van Leeuwen RE, Schellings MW, Barenbrug P, Maessen JG, Heymans S, Pinto YM, Creemers EE. miR-133 and miR-30 regulate connective tissue growth factor: implications for a role of microRNAs in myocardial matrix remodeling. *Circ Res*. 2009; **104**: 170–178 176p following 178.
18. Da Costa Martins PA, De Windt LJ. MicroRNAs in control of cardiac hypertrophy. *Cardiovascular Research*. 2012; **93**: 563–572.
19. Verbeek XA, Vernooy K, Peschar M, Cornelussen RN, Prinzen FW. Intra-ventricular resynchronization for optimal left ventricular function during pacing in experimental left bundle branch block. *Journal of the American College of Cardiology*. 2003; **42**: 558–567.
20. Arts T, Prinzen FW, Delhaas T, Milles JR, Rossi AC, Clarysse P. Mapping displacement and deformation of the heart with local sine-wave modeling. *IEEE Transactions on Medical Imaging*. 2010; **29**: 1114–1123.
21. Verbeek XA, Vernooy K, Peschar M, Van Der Nagel T, Van Hunnik A, Prinzen FW. Quantification of interventricular asynchrony during LBBB and ventricular pacing. *American Journal of Physiology Heart and Circulatory Physiology*. 2002; **283**: H1370–H1378.
22. de Jong S, van Middendorp LB, Hermans RH, de Bakker JM, Bierhuizen MF, Prinzen FW, van Rijen HV, Losen M, Vos MA, van Zandvoort MA. Ex vivo and in vivo administration of fluorescent CNA35 specifically marks cardiac fibrosis. *Molecular Imaging*. 2014; **13**: 1–9.
23. Vernooy K, Cornelussen RN, Verbeek XA, Vanagt WY, van Hunnik A, Kuiper M, Arts T, Crijns HJ, Prinzen FW. Cardiac resynchronization therapy cures dyssynchronopathy in canine left bundle-branch block hearts. *European Heart Journal*. 2007; **28**: 2148–2155.
24. Fontes MS, Kessler EL, van Stuijvenberg L, Brans MA, Falke LL, Kok B, Leask A, van Rijen HV, Vos MA, Goldschmeding R, van Veen TA. CTGF knockout does not affect cardiac hypertrophy and fibrosis formation upon chronic pressure overload. *Journal Of Molecular and Cellular Cardiology*. 2015; **88**: 82–90.
25. Accornero F, van Berlo JH, Correll RN, Elrod JW, Sargent MA, York A, Rabinowitz JE, Leask A, Molkentin JD. Genetic analysis of connective tissue growth factor as an effector of transforming growth factor beta signaling and cardiac remodeling. *Molecular and Cellular Biology*. 2015; **35**: 2154–2164.
26. Marfella R, Di Filippo C, Potenza N, Sardu C, Rizzo MR, Siniscalchi M, Musacchio E, Barbieri M, Mauro C, Mosca N, Solimene F, Mottola MT, Russo A, Rossi F, Paolisso G, D'Amico M. Circulating microRNA changes in heart failure patients treated with cardiac resynchronization therapy: responders vs. non-responders. *European Journal of Heart Failure*. 2013; **15**: 1277–1288.
27. De Boeck BW, Kirn B, Teske AJ, Hummeling RW, Doevendans PA, Cramer MJ, Prinzen FW. Three-dimensional mapping of mechanical activation patterns, contractile dyssynchrony and dyscoordination by two-dimensional strain echocardiography: rationale and design of a novel software toolbox. *Cardiovascular Ultrasound*. 2008; **6**: 22.
28. Wyman BT, Hunter WC, Prinzen FW, Faris OP, McVeigh ER. Effects of single- and biventricular pacing on temporal and spatial dynamics of ventricular contraction. *American Journal of Physiology Heart and Circulatory Physiology*. 2002; **282**: H372–H379.
29. Melman YF, Shah R, Danielson K, Xiao J, Simonson B, Barth A, Chakir K, Lewis GD, Lavender Z, Truong QA, Kleber A, Das R, Rosenzweig A, Wang Y, Kass DA, Singh JP, Das S. Circulating MicroRNA-30d is associated with response to cardiac resynchronization therapy in heart failure and regulates cardiomyocyte apoptosis: a translational pilot study. *Circulation*. 2015; **131**: 2202–2216.
30. Russell K, Eriksen M, Aaberge L, Wilhelmsen N, Skulstad H, Gjesdal O, Edvardsen T, Smiseth OA. Assessment of wasted myocardial work: a novel method to quantify energy loss due to uncoordinated left ventricular contractions. *American Journal of Physiology Heart and Circulatory Physiology*. 2013; **305**: H996–1003.